ACS Medicinal Chemistry Letters

Letter

pubs.acs.org/acsmedchemlett

Novel Hybrid-Type Antimicrobial Agents Targeting the Switch Region of Bacterial RNA Polymerase

Fumika Yakushiji,*[,†] Yuko Miyamoto,[†] Yuki Kunoh,[†] Reiko Okamoto,[†] Hidemasa Nakaminami,[‡] Yuri Yamazaki,[†] Norihisa Noguchi,[‡] and Yoshio Hayashi*[,†]

Departments of [†]Medicinal Chemistry and [‡]Microbiology, School of Pharmacy, Tokyo University of Pharmacy and Life Sciences, 1432-1 Horinouchi, Hachioji, Tokyo 192-0392, Japan

Supporting Information

ABSTRACT: The bacterial RNA polymerase (RNAP) is an ideal target for the development of antimicrobial agents against drug-resistant bacteria. Especially, the switch region within RNAP has been considered as an attractive binding site for drug discovery. Here, we designed and synthesized a series of novel hybrid-type inhibitors of bacterial RNAP. The antimicrobial activities were evaluated using a paper disk diffusion assay, and selected derivatives were tested to determine their MIC values. The hybrid-type antimicrobial agent **29** showed inhibitory activity against *Escherichia coli* RNAP. The molecular docking study suggested that the RNAP switch region would be the binding site of **29**.

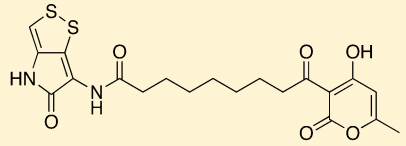

Hybrid-type antimicrobial agent **29**
Inhibitory activity against *E. coli* RNA polymerase

KEYWORDS: *bacterial RNA polymerase, switch region, antimicrobial agent, bacterial RNA polymerase inhibitor, hybrid*

Rifamycins are a class of bacterial RNA polymerase (RNAP) inhibitors commonly used in clinical practice. The potency and broad-spectrum nature of rifamycins have improved the treatment of infectious diseases, including tuberculosis. Nevertheless, the emergence of drug-resistant bacteria poses an ongoing threat to the therapeutic index of rifamycins. For this reason, the development of a novel RNAP inhibitor is in demand. In 2008, a research team led by Arnold and Ebright elucidated the inhibitory mechanism of myxopyronin A (**1**) (Figure 1),[1] which was targeting the switch region of bacterial RNAP, and an X-ray crystal structure of **1** in complex with *T. thermophilus* RNAP was reported.[2,3] Corallopyronin (**3**) and ripostatins also appeared to bind to the RNAP switch region.[2] Hence, this newly identified binding site in RNAP has attracted the attention of medicinal chemists to develop new antimicrobial agents.

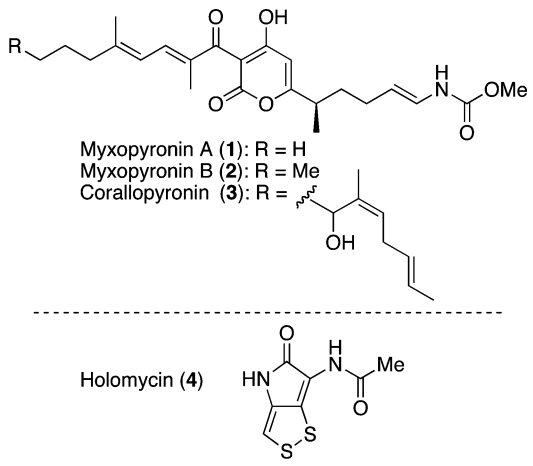

Figure 1. Structures of antibiotics myxopyronins A (**1**) and B (**2**), corallopyronin (**3**), and holomycin (**4**).

Before now, the research group of Simonsen and Xiang attempted a direct structure−activity relationship study of myxopyronin.[4,5] In addition, Fishwick and co-workers tried structure-based ligand design at the myxopyronin binding site.[6] On the other hand, Moy and co-workers reported that myxopyronin was an unsuitable lead compound for medicinal development because of the high binding to serum albumin, the low stability, and the occurrence of resistant strains.[7]

In this report, we disclose our effort to develop novel antimicrobial agents with a hybrid strategy[8,9] for myxopyronin derivatives. To enhance the antimicrobial activity, reduce the lipophilicity, and improve the instability, the antibiotic holomycin (**4**)[10] was incorporated into the mother skeleton of the myxopyronin-type RNAP inhibitors.

Holomycin (**4**) also possessed antibacterial properties and provided moderate but broad antibiotic spectrum against Gram-positive and -negative bacteria.[11,12] In addition, **4** showed the inhibition of RNA synthesis,[11] and the calculate log P (ClogP) did not exceed 2.0.[13] These properties fascinated us to hybridize myxopyronins with the holothin molecule to expect the efficacy beyond our anticipations.

Our hybrid strategy is shown in Figure 2. We designed two types of hybrid derivatives based on the reported X-ray crystal structure of RNAP with **1** (PDB: 3DXJ).[2,3] One was the "right-hand amide derivative (**6**)" with the core α-pyrone at the center and the holothin component positioned on the right-hand side. Toward the right side of the X-ray crystal structure, as shown in the blue circle in Figure 2, there is an intermolecular hydrogen

Received: October 17, 2012
Accepted: December 30, 2012
Published: January 11, 2013

dx.doi.org/10.1021/ml300350p | ACS Med. Chem. Lett. 2013, 4, 220−224

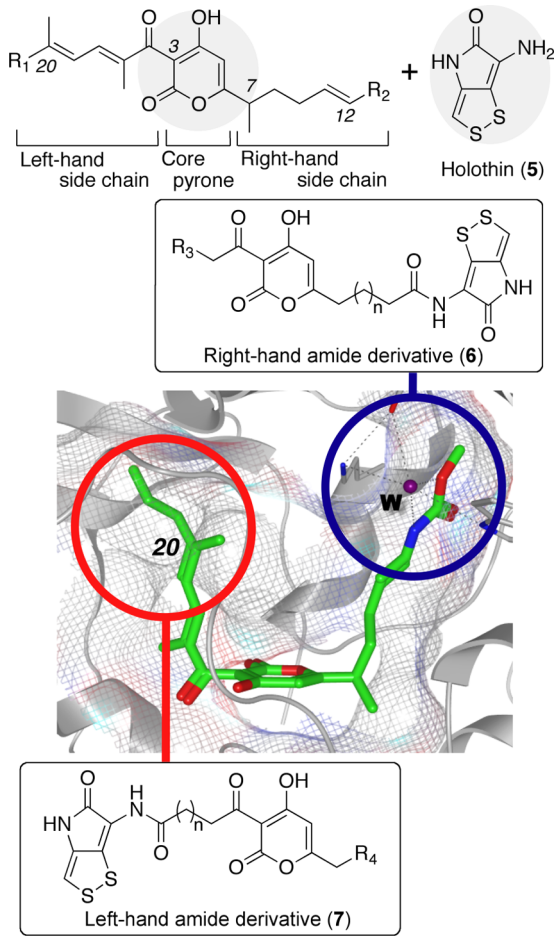

Figure 2. Design of hybrid-type derivatives including core α-pyrone and holothin (**5**) based on the X-ray crystallography of **1** within bacterial RNAP from *T. thermophilus* (PDB: 3DXJ; green stick, myxopyronin A; gray stick and ribbon, bacterial RNAP; gray mesh, myxopyronin binding site; W, water molecule; blue circle, intermolecular hydrogen bond network at the right-hand side; and red circle, space at the left-hand side).

bond network involving a water molecule. The holothin (**5**), which included several heteroatoms, was incorporated into the right-hand moiety to form the hydrogen bonds. The other is the "left-hand amide derivative (**7**)". The holothin was introduced at the left side of the molecule relative to the C3 side chain. At the left side of the myxopyronin binding site, as shown in the red circle in Figure 2, there is a useful space around the C20 hydrocarbon chain. This interspace was advantageous for accommodating the holothin moiety to increase the interaction with RNAP.

We first synthesized right-hand amide derivatives (Scheme 1). The C3-acylation of starting material **8** proceeded in the presence of propionic acid via condensation and rearrangement to obtain **9**.[14] The pyrone **9** was alkylated with **10**,[15] then the silyl protecting group was removed, and two-step oxidation produced the carboxylic acid **11**.[4] Compound **11** was treated with oxalyl chloride and condensed with holothin hydrochloride **12**[16] under basic conditions to yield the simplified hybrid derivative **13**. On the other hand, **17** was synthesized to ascertain the importance of the left-hand portion of the hybrid compound. Compound **8** was acylated with nonanoic acid, and the resultant pyrone **14** was converted to a carboxylic acid **16** through the same four steps. Compound **16** was condensed with the holothin salt **12** to construct the desired **17**. We attempted to prepare a series of right-hand derivatives with unsaturated carbon side chains; however, the final products could not be isolated due to decomposition at the purification step. These observations suggested that the unsaturated side chain of **1** was one factor for the reported instability.[7]

We next attempted to synthesize the left-hand amide derivatives. As shown in Scheme 2A, **8** and different lengths of the hydrocarbon linkers **18**–**20** were treated with *N*,*N*′-diisopropylcarbodiimide (DIC) and DMAP for the C3-acylation.[14] The methyl ester groups of the obtained **21**–**23** were then hydrolyzed to the carboxylic acids **24**–**26**, followed by the condensation of **24**–**26** with **12** to generate **27**–**29**. Compound **28** was subsequently converted to the sulfone **30** using oxone as the oxidizing reagent.[17,18]

The synthetic route B (Scheme 2B) showed the synthesis of the derivative **32** including the right-hand alkyl chain and the left-hand amide part. Compound **8** was alkylated using 4-

Scheme 1. Syntheses of the Right-Hand Amide Derivatives 13 and 17[a]

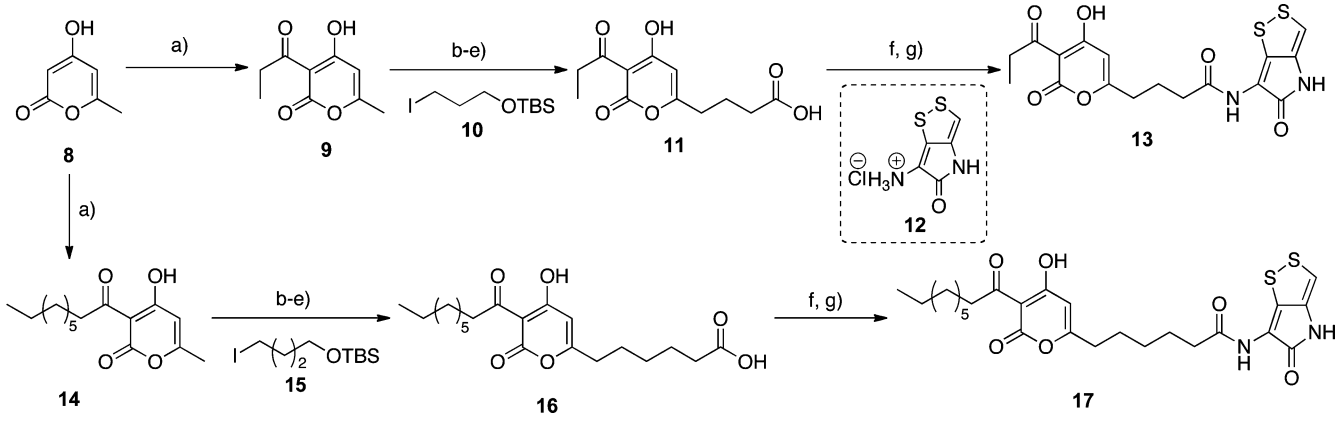

[a]Reagents and conditions: (a) Propionic acid or nonanoic acid, DIC, DMAP, toluene, 100 °C, 5 or 14 h, 72 or 74%, respectively. (b) Compound **10** or **15**, LDA, HMPA, THF, −78 °C, 1 h, 75%. (c) AcOH/THF/H_2O (3/1/1), rt, 26 h, 66–89%. (d) PCC, CH_2Cl_2, rt, 30 min. (e) $NaClO_2$, NaH_2PO_4, 2-methyl-2-butene, ^{t}BuOH/THF/H_2O (1/1/1), rt, 4 h, 63–84%. (f) $(COCl)_2$, toluene, rt, 1 h. (g) Compound **12**, Et_3N, THF/toluene, rt, 30 min, 61–65%.

dx.doi.org/10.1021/ml300350p | *ACS Med. Chem. Lett.* 2013, 4, 220–224

Scheme 2. Syntheses of the Left-Hand Amide Derivatives 27−29, 30, 32, and 35[a]

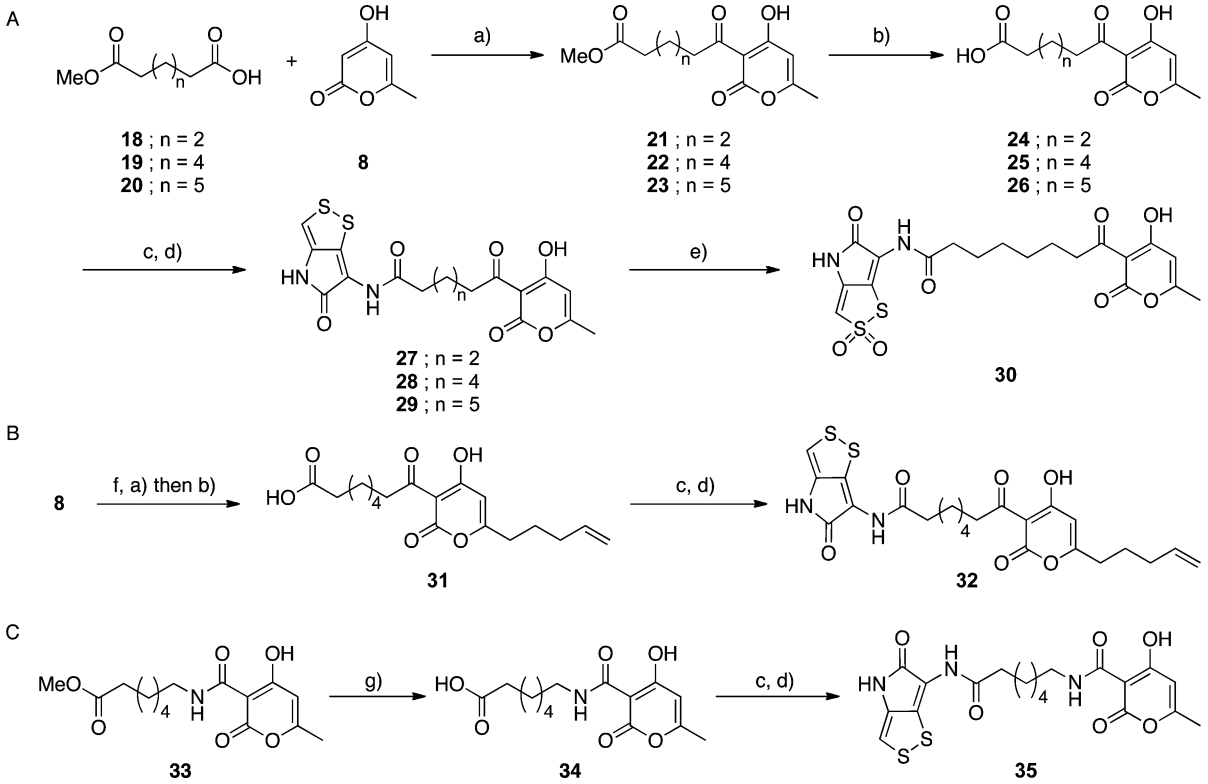

[a]Reagents and conditions: (a) Compound **18**, **19**, or **20**, DIC, DMAP, toluene, 100 °C, 6−14 h, 64−93%. (b) 1 M LiOH aq/THF (1/4), rt, 14 h. (c) $(COCl)_2$, toluene, rt, 1 h. (d) Compound **12**, Et_3N, THF/toluene, rt, 30 min, 38−66%. (e) Oxone, acetone/H_2O, 0 °C, 30 min, 40%. (f) 4-Bromo-1-butene, LDA, HMPA, THF, rt, 14 h, 85%. (g) $Ba(OH)_2$, H_2O/THF, 73 °C, 2 h.

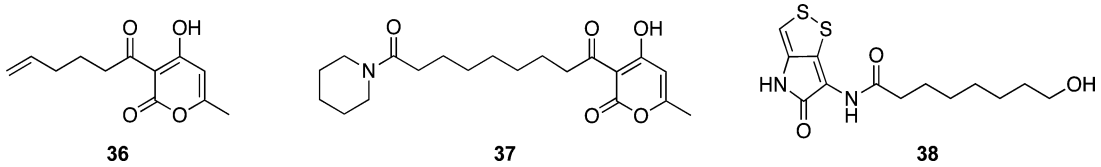

Figure 3. Structures of the synthesized derivatives **36−38**.

bromo-1-butene, and the C3 position of the obtained pyrone was acylated with **19**. After hydrolysis, the resultant carboxylic acid **31** was condensed with **12** to obtain **32**.

The synthetic route C (Scheme 2C) describes the preparation of a C3 amide derivative. The amide ester analogue **33**, prepared from 4-hydroxy-6-methyl-2-oxo-2*H*-pyran-3-carboxylic acid[19] and methyl 7-aminoheptanoate, was mildly hydrolyzed to **34**, and then, the carboxylic acid was condensed with **12** to synthesize the product **35**.

As other derivatives, three compounds **36−38** were also synthesized (Figure 3).[20] Compound **36** was constructed to ascertain the significance of the length of the left-hand hydrocarbon linker. The piperidine-containing derivative **37** was synthesized to examine the effect of the holothin component. The holothin derivative **38**[21] was also synthesized to observe the efficacy of a hybrid structure including α-pyrone.

The synthesized derivatives were evaluated as an antimicrobial agent using a simple paper disk diffusion assay against *Bacillus subtilis* (Table 1).[22] The right-hand amide derivatives were tested first. The synthetic intermediate **9** did not exhibit a zone of inhibition. The right-hand amide derivative **13** also showed no antimicrobial activity. By contrast, **14**, **16**, and **17**, which included left-hand side chains, produced inhibition zones. These results suggested that the left-hand side chain played an important role in the antimicrobial activity. Furthermore, it became clear that the antimicrobial properties of this series did not depend on the holothin moiety.

Table 1. Disk Diffusion Assay against *B. subtilis*

compd[a]	inhibition zone[b] (mm)	compd[a]	inhibition zone[b] (mm)
9	no zone	**31**	no zone
13	no zone	**32**	10
14	12	**34**	no zone
16	slight	**35**	slight
17	9	**36**	9
25	no zone	**37**	no zone
27	14	**38**	9
28	11	RFP	25
29	15	(±)-**2**	slight
30	no zone	MeOH	no zone

[a]All compounds were dissolved in MeOH and evaluated at a dose of 30 μg/disk. [b]Diameter of zones with complete growth inhibition.

dx.doi.org/10.1021/ml300350p | *ACS Med. Chem. Lett.* 2013, 4, 220−224

Next, left-hand amide derivatives were evaluated. As compared with the carboxylic acid **25** and the hybrid derivatives **27**−**29**, the hybrid-type derivatives showed zones of inhibition. These results suggested that the presence of the holothin moiety enhanced the activity. Compound **30**, including a sulfone group, and **31** and **32** with right-hand hydrocarbon chains were compared with **28**; however, these derivatives did not show significant validity, suggesting that the sulfone group and the right-hand chains did not contribute to the activity. Furthermore, **34** did not show any activity, although **35** exhibited a slight zone of inhibition. The α-pyrone **36** and the holothin derivative **38** showed weak activities, whereas **37** produced no zone of inhibition. The synthesized (±)-myxopyronin B[15] was also tested; however, (±)-**2** produced only a slight zone of inhibition in our assay system. Therefore, the authentic rifampicin (RFP) was used as a standard antibiotic in all assays.

The results in Table 1 indicated that the C3 position of the α-pyrone should be substituted with a long hydrocarbon moiety for the expression of the antimicrobial activity. In addition, the hybrid derivatives containing α-pyrone and the holothin moiety exhibited the enhanced activity.

On the basis of results of the paper disk assay, we selected the effective derivatives **14**, **27**, and **29** for the next evaluations of higher order assessments. These simplified derivatives presented larger zones of inhibition, small molecular weights, and low lipophilicities, as assessed by ClogP.[13]

The minimal inhibitory concentration (MIC) was evaluated to characterize the antimicrobial activity of **14**, **27**, and **29** against eight kinds of Gram-positive and -negative bacteria and fungi (Table 2). After 24 h of incubation, α-pyrone-type

Table 2. MIC Values for Selected Derivatives 14, 27, and 29

	MIC (μg/mL)			
organism	**14**	**27**	**29**	RFP
Staphylococcus aureus ATCC29213	8	64	4	0.5
Enterococcus faecalis ATCC29212	4	16	4	1
M. luteus ATCC9341	2	8	1	≤0.125
B. subtilis ATCC6633	8	64	16	≤0.125
E. coli ATCC25922	128	128	≥256	8
Pseudomonas aeruginosa ATCC27853	128	64	128	32
Serratia marcescens ATCC13880	128	128	≥256	32
Candida albicans ATCC10231	64	128	≥256	≥256

derivative **14**[23] and the hybrid-type derivative **29** showed good antimicrobial activity against Gram-positive bacteria, although the activity against Gram-negative bacteria and fungi was weak. The extension of the left-hand chain was effective for the inhibition against the Gram-positive bacteria. Furthermore, **14**, **27**, and **29** gave the strongest activity against *Micrococcus luteus*. The selective inhibitory activity against bacteria would depend on our hybrid derivatives.

Besides, **14**, **27**, and **29** were evaluated for their in vitro inhibitory activity against *Escherichia coli*. RNAP (Table 3). The derivative **29** inhibited *E. coli* RNAP, and the IC_{50} value was determined to be 14 ± 1.7 μM. Unfortunately, **14** and **27** did not exhibit inhibitory activity. The IC_{50} value of **29** was higher than that of RFP, but the difference of activities might be a result of the binding site recognition.[3] In addition, the ineffectiveness of **29** against *E. coli* in MIC might be due to the low penetration ability in Gram-negative bacteria. However,

Table 3. In Vitro Inhibitory Activity against *E. coli* RNA Polymerase

compd	IC_{50} (μM)[a,b]
14	>2 mM
27	>2 mM
29	14 ± 1.7
RFP	0.08 ± 0.01

[a]IC_{50} values are means ± SEMs from three independent dose−response curves, in which each measurement was done in duplicate. [b]The reported IC_{50} values of myxopyronin B were 46.5[6] and 24[7] μM, respectively.

the results in Table 3 suggested that the target of **29** was the bacterial RNAP.

From the above, the expected binding site of **29** in RNAP was considered in a molecular docking study based on X-ray crystal data of myxopyronin A and RNAP complex (PDB: 3DXJ).[24] As shown in Figure 4, **29** showed good conformation

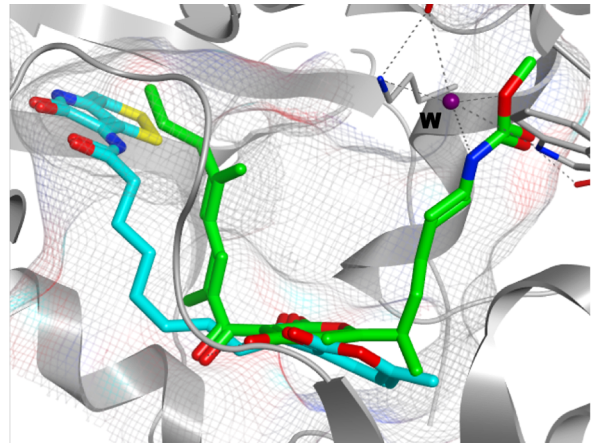

Figure 4. Molecular docking study of **29** in the switch region of *T. thermophilus* RNAP (PDB: 3DXJ). Binding energy, −8.3 kcal/mol (blue stick, **29**; green stick, myxopyronin A; gray stick and ribbon, bacterial RNAP; gray mesh, myxopyronin binding site; and W, water molecule).

in the hydrophobic pocket of the switch region with a minimum binding energy of −8.3 kcal/mol. Other predicted conformations of **29** within RNAP were also examined; however, these provided high binding energies over 13 kcal/mol at least. Consequently, the expected binding site of **29** within RNAP would be regarded as the switch region.

In summary, we designed and synthesized hybrid-type antimicrobial derivatives including the core α-pyrone and the holothin moiety toward the development of novel bacterial RNAP inhibitors. The simplified derivative **29**, in particular, showed reliable antimicrobial activity against Gram-positive bacteria. Furthermore, **29** inhibited *E. coli* RNAP, and the molecular docking study suggested that the targeted switch region would be the binding site. Our hybrid strategy revealed that the left-hand moiety of the α-pyrone component had a great effect on the antimicrobial activity, and the inserted holothin part enhanced the ability. In addition, a derivative with low lipophilicity and inhibitory activity against bacterial RNAP was identified. Significantly, selectivity of antimicrobial action and profiles of our hybrid-type derivatives indicated the unexpected validity of hybridization. Hence, the hybrid strategy would be one of the effective ways to explore novel drug

dx.doi.org/10.1021/ml300350p | ACS Med. Chem. Lett. 2013, 4, 220−224

candidates. The structure−activity relationship study of the simplified derivatives and the X-ray crystallographic analysis of the cocrystal (**29** and bacterial RNAP) are in progress.

■ ASSOCIATED CONTENT

Supporting Information

General information, details of the compound syntheses and characterization, and the biological assay protocols. This material is available free of charge via the Internet at http://pubs.acs.org.

■ AUTHOR INFORMATION

Corresponding Author

*Tel: 81-42-676-3279. Fax: 81-42-676-4475. E-mail: fyakushi@toyaku.ac.jp. E-mail: yhayashi@toyaku.ac.jp.

Funding

This research was supported by grants from MEXT (the Ministry of Education, Culture, Sports, Science and Technology), Japan, including the Platform for Drug Discovery, Informatics, and Structural Life Science, the Grant-in-Aid for Research Activity Start-up (No. 21890262), and the Grant-in-Aid for Young Scientists (B) (No. 23790142).

Notes

The authors declare no competing financial interest.

■ ACKNOWLEDGMENTS

We thank C. Sakuma of Tokyo University of Pharmacy and Life Sciences for NMR and mass spectroscopy measurements.

■ REFERENCES

(1) Irschik, H.; Gerth, K.; Höfle, G.; Kohl, W.; Reichenbach, H. The myxopyronins, new inhibitors of bacterial RNA synthesis from *Myxococcus fulvus* (Myxobacterales). *J. Antibiot.* **1983**, *36*, 1651−1658.

(2) Mukhopadhyay, J.; Das, K.; Ismail, S.; Koppstein, D.; Jang, M.; Hudson, B.; Sarafianos, S.; Tuske, S.; Patel, J.; Jansen, R.; Irschik, H.; Arnold, E.; Ebright, R. H. The RNA polymerase "switch region" is a target for inhibitors. *Cell* **2008**, *135*, 295−307.

(3) Ho, M. X.; Hudson, B. P.; Das, K.; Arnold, E.; Ebright, R. H. Structures of RNA polymerase-antibiotic complexes. *Curr. Opin. Struct. Biol.* **2009**, *19*, 715−723.

(4) Doundoulakis, T.; Xiang, A. X.; Lira, R.; Agrios, K. A.; Webber, S. E.; Sisson, W.; Aust, R. M.; Shah, A. M.; Showalter, R. E.; Appleman, J. R.; Simonsen, K. B. Myxopyronin B analogs as inhibitors of RNA polymerase, synthesis and biological evaluation. *Bioorg. Med. Chem. Lett.* **2004**, *14*, 5667−5672.

(5) Lira, R.; Xiang, A. X.; Doundoulakis, T.; Biller, W. T.; Agrios, K. A.; Simonsen, K. B.; Webber, S. E.; Sisson, W.; Aust, R. M.; Shah, A. M.; Showalter, R. E.; Banh, V. N.; Steffy, K. R.; Appleman, J. R. Syntheses of novel myxopyronin B analogs as potential inhibitors of bacterial RNA polymerase. *Bioorg. Med. Chem. Lett.* **2007**, *17*, 6797−6800.

(6) McPhillie, M. J.; Trowbridge, R.; Mariner, K. R.; O'Neill, A. J.; Johnson, A. P.; Chopra, I.; Fishwick, C. W. G. Structure-based ligand design of novel bacterial RNA polymerase inhibitors. *ACS Med. Chem. Lett.* **2011**, *2*, 729−734.

(7) Moy, T. I.; Daniel, A.; Hardy, C.; Jackson, A.; Rehrauer, O.; Hwang, Y. S.; Zou, D.; Nguyen, K.; Silverman, J. A.; Li, Q.; Murphy, C. Evaluating the activity of the RNA polymerase inhibitor myxopyronin B against *Staphylococcus aureus*. *FEMS Microbiol. Lett.* **2011**, *319*, 176−179.

(8) See the review: Tietze, L. F.; Bell, H. P.; Chandrasekhar, S. Natural product hybrids as new leads for drug discovery. *Angew. Chem., Int. Ed.* **2003**, *42*, 3996−4028.

(9) Tsogoeva, S. B. Recent progress in the development of synthetic hybrids of natural or unnatural bioactive compounds for medicinal chemistry. *Mini Rev. Med. Chem.* **2010**, *10*, 773−793.

(10) Kenig, M.; Reading, C. Holomycin and an antibiotic (MM19290) related to tunicamycin, metabolites of *Streptomyces clavuligerus*. *J. Antibiot.* **1979**, *32*, 549−554.

(11) Oliva, B.; O'Neill, A.; Wilson, J. M.; O'Hanlon, P. J.; Chopra, I. Antimicrobial properties and mode of action of the pyrrothine holomycin. *Antimicrob. Agents Chemother.* **2001**, *45*, 532−539.

(12) O'Neill, A.; Oliva, B.; Storey, C.; Hoyle, A.; Fishwick, C.; Chopra, I. RNA polymerase inhibitors with activity against rifampin-resistant mutants of *Staphylococcus aureus*. *Antimicrob. Agents Chemother.* **2000**, *44*, 3163−3166.

(13) The value of calculate Log P (ClogP) was calculated by CS ChemBioDraw Ultra 12.0 (Cambridgesoft.com).

(14) Mori, T.; Ujihara, K.; Matsumoto, O.; Yanagi, K.; Matsuo, N. Synthetic studies of fluorine-containing compounds for household insecticides. *J. Fluorine Chem.* **2007**, *128*, 1174−1181.

(15) Hu, T.; Schaus, J. V.; Lam, K.; Palfreyman, M. G.; Wuonola, M.; Gustafson, G.; Panek, J. S. Total synthesis and preliminary antibacterial evaluation of the RNA polymerase inhibitors (±)-myxopyronin A and B. *J. Org. Chem.* **1998**, *63*, 2401−2406.

(16) Compound **12** was synthesized according to the following manuscript. Hjelmgaard, T.; Givskov, M.; Nielsen, J. Expedient total synthesis of pyrrothine natural products and analogs. *Org. Biomol. Chem.* **2007**, *5*, 344−348.

(17) Adam, W.; Chan, Y.-Y.; Cremer, D.; Gauss, J.; Scheutzow, D.; Schindler, M. Spectral and chemical properties of dimethyldioxirane as determined by experiment and ab initio calculations. *J. Org. Chem.* **1987**, *52*, 2800−2803.

(18) Yu, B.; Liu, A.-H.; He, L.-N.; Li, B.; Diao, Z.-F.; Li, Y.-N. Catalyst-free approach for solvent-dependent selective oxidation of organic sulfides with oxone. *Green Chem.* **2012**, *14*, 957−962.

(19) Suzuki, E.; Sekizaki, H.; Inoue, S. A new and simple synthesis of triacetic acid lactone-3-carboxylic acid (3-carboxy-4-hydroxy-6-methyl-2-pyrone). *Synthesis* **1975**, 652−653.

(20) See the Supporting Information.

(21) Shiozawa, H.; Kagasaki, T.; Kinoshita, T.; Haruyama, H.; Domon, H.; Utsui, Y.; Kodama, K.; Takahashi, S. Thiomarinol, a new hybrid antimicrobial antibiotic produced by a marine bacterium fermentation, isolation, structure, and antimicrobial activity. *J. Antibiot.* **1993**, *46*, 1834−1842.

(22) National Committee for Laboratory Standards. *Performance Standards for Antimicrobial Disk Susceptibility Tests*; Approved standard M2-A8; NCCLS: Wayne, 2003.

(23) The similar derivative of **14**, 4-hydroxy-6-methyl-3-octanoyl-2*H*-pyran-2-one, was reported as an antibacterial agent. Ukita, T.; Mizuno, D.; Tamura, T.; Yamakawa, T.; Nojima, S. The antibacterial properties of compounds containing the tricarbonylmethane group. II-III. Antibacterial properties of 3-alkylated or 3-acylated 4-hydroxycoumarins and of a related pyrone. *J. Pharm. Soc. Jpn.* **1951**, *71*, 234−243.

(24) The molecular docking study was performed using the molecular modeling package MOE 2010.10 (Chemical Computing Group, Inc., Montreal, Canada).